The numerical investigation of Effects of Darcy and Forchheimer parameters on Magnetohydrodynamic Casson fluid flow through non-Darcy porous media

Bhim Sen Kala

Department of Mathematics, K L University, Guntur, 522502, Andhra Pradesh, India

Abstract *---In the present paper we investigate numerically the effect of Darcy and Forchheimer parameters on Magnetohydrodynamic Casson fluid flow. By suitable similarity transformations, the governing boundary layer equations are transformed to ordinary differential equations and to solve these equations the method applied is numerical computation with bvp4c, a MATLAB program. The effects of Casson fluid parameter,Magnetic Parameter, Darcy Parameter, and Forcheimer parameter on velocity, heat transfer, and concentration profiles, Skin- Frictions, Nusselt Number and Sherwood Number are computed and discussed numerically and presented through tables and graphs.*

Keywords--- *Magnetohydrodynamic fluid flow, Darcy parameter, Forchheimer parameter, Casson fluid.*

1. INTRODUCTION

Many natural, industrial as well as biological fluids such as mud, condensed milk, glues, lubricating greases, multi grade oils, gypsum pastes, emulsions, paints, sugar solution, shampoos and tomato paste, ceramics, polymers, liquid detergents, blood, fruit juices etc. change their viscosity or flow behaviour under stress and thus deviate from the classical Newton's law of viscosity. Different models of non-Newtonian fluids based on their diverse flow behaviours have been proposed by the researchers.

The rheological model was introduced originally by Casson [1] in his research on a flow equation for pigment oil-suspensions of printing ink. Bird et al. [2] investigated the rheology and flow of visco-plastic materials and reported that Casson model constitutes a plastic fluid model which exhibits shear thinning characteristics, yield stress, and high shear viscosity. Casson fluid behaves as solid when the shear stress is less than the yield stress and it starts to deform when shear stress becomes greater than the yield stress.

The fundamental analysis of the flow field of non-Newtonian fluids in a boundary layer adjacent to a stretching sheet or an extended surface is very important and is an essential part in the study of fluid dynamics and heat and mass transfer.

Sakiadis, B.C.[3]studied boundary layer behaviour on continuous solid surfaces: II. The boundary layer on continuous flat surface. Crane L.J.[4] studied the Flow past a stretching plane. Nield, D.A.et al.[5] studied Convection in porous media.

Mukhopadhyay, S [6] investigated Casson fluid flow and heat transfer over a nonlinearly stretching surface. Mustafa, M. et al. [7] studied Model for flow of Casson nanofluid past a non-linearly stretching sheet considering magnetic field effects. Medikare, M., et al.[8] studied MHD

Stagnation Point Flow of a Casson Fluid over a Nonlinearly Stretching Sheet with Viscous Dissipation.

Pramanik, S. [9] studied Casson fluid flow and heat transfer past an exponentially porous stretching surface in presence of thermal radiation. Raju, C.S.K. et al.[10] studied Heat and mass transfer in magnetohydrodynamic Casson fluid over an exponentially permeable stretching surface. Saidulu, N. et al. [11] studied Slip Effects on MHD Flow of Casson Fluid over an Exponentially Stretching Sheet in Presence of Thermal Radiation, Heat Source/Sink and Chemical Reaction. . Sharada, K. et al. [12] studied MHD Mixed Convection Flow of a Casson Fluid over an Exponentially Stretching Surface with the Effects of Soret, Dufour, Thermal Radiation and Chemical Reaction. Mukhopadhyay,Swati et al [13] studied Exact solutions for the flow of Casson fluid over a stretching surface with transpiration and heat transfer effects. Hayat et al. [14] investigated Soret and Dufour effects on magnetohydrodynamic (MHD) flow of Casson fluid. Mahdy, A.[15] studied heat transfer and flow of a Casson fluid due to a stretching cylinder with the Soret and Dufour effects. Animasaun, I.L. [16] studied Effects of thermophoresis, variable viscosity and thermalconductivity on free convective heat and mass transfer of non-Darcian MHD dissipative Casson fluid flow with suction and nth order of chemical reaction .

Ullah, I., Sharidan et al. [17] investigated Effects of slip condition and Newtonian heating on MHD flow of Casson fluid over a nonlinearly stretching sheet saturated in a porous medium.

Some recent studies concerning the flow, heat and mass transfer analysis of Casson fluid can be found in Refs. 18–25.

We consider (1) non Darcy porous medium, (2)thermo –diffusion(Dufour term) term in energy equation, (3)including mass equations,(4)diffusion -thermo term(Soret term) in the mass equation and (5)velocity slip factor, thermal slip factor, and mass slip factor in boundary conditions of velocity, temperature, and concentration respectively . In the above work these terms, simultaneously in one problem, are not investigated with the flow over nonlinear surface.

The present work is the extension of Ullah, I., Sharidan et al. [17] work by considering above terms. In it, we investigate numerically the Effects of Darcy and Forchheimer parameters on Magnetohydrodynamic Casson fluid flow through non Darcy porous media.

II. MATHEMATICAL FORMULATION OF THE PROBLEM

In the formulation of the problem we consider following assumptions. Casson fluid is incompressible and electrically conducting. Flow is steady, laminar and two dimensional over a nonlinearly stretching sheet. Flow region is in non-Darcy porous medium. It is under the influence of transverse magnetic field B.The sheet is stretched nonlinearly along the x-axis (i.e. y=0)with velocity $u_w(x) = c\,x^n$;origin is taken as fixed and the fluid flow is confined to y>0. Here c is constant and $n(n \geq 0)$ is the nonlinear stretching sheet parameter; $n=1$ represents the linear sheet case and $n \neq 1$ is for nonlinear case. The magnetic Reynolds number of the flow is taken to be small enough so that induced magnetic field is assumed to be negligible in comparison with applied magnetic field so that $B=(0, B(x), 0)$, where $B(x)$ is the applied magnetic field acting normal to the plate and varies in strength as a function of x. The flow is assumed to be in the x-direction which is taken along the plate and y-axis is normal to it. There is a constant suction/injection velocity v_w normal to the plate.

Under these assumptions the rheological equation for incompressible flow of Casson fluid is given by (Sharada et al. [12], Mukhopadhyay,S. ,et al.[13])

$$\tau_{ij} = \begin{cases} 2(\mu_B + p_y/\sqrt{2\pi})e_{ij} & \pi > \pi_c\,, \\ 2(\mu_B + p_y/\sqrt{2\pi_c})e_{ij} & \pi < \pi_c \end{cases}.$$

where $\pi = e_{ij}\,e_{ij}$ and e_{ij} is the $(i,i)-$th component of the deformation rate , π is the product of the components of deformation , π_c is critical value of the product based on the non-Newtonian model, μ_B is the plastic dynamic viscosity of the non-Newtonian fluid, and p_y is the yield stress of the fluid. The viscosity and thermal conductivity of the fluid are assumed to be constant. There is thermo-diffusion effect as well as diffusion-thermo effect. The pressure gradient, body forces and Joule heating are neglected compared with the effect of viscous dissipation. The temperature and concentration of the stretching surface are always greater than their free stream values. The flow configuration and the coordinate system are shown in Figure 1.

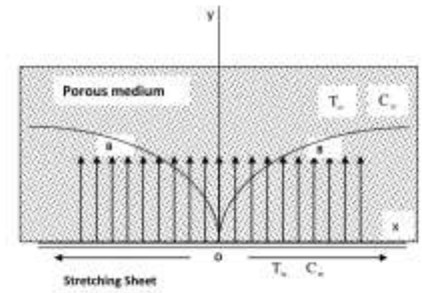

Figure 1 Physical model and coordinate system.

Under the above assumptions and using Bossinesqu approximation, boundary layer equations for flow with heat and mass transfer in casson fluid are given by the following.

The continuity equation:

$$\frac{\partial u}{\partial x} + \frac{\partial v}{\partial y} = 0\,,$$

(1)

The equation of momentum:

$$u\frac{\partial u}{\partial x} + v\frac{\partial u}{\partial y} = \upsilon\left(1+\frac{1}{\beta}\right)\frac{\partial^2 u}{\partial y^2} + g\beta_T(T-T_\infty)$$
$$+ g\beta_C(C-C_\infty) - \frac{\sigma B^2(x)}{\rho}u - \frac{\upsilon}{K}u - \frac{b}{\sqrt{K}}u^2$$

(2)

Energy Equation:

$$u\frac{\partial T}{\partial x} + v\frac{\partial T}{\partial y} = \alpha\frac{\partial^2 T}{\partial y^2} + \left(\frac{D_m K_T}{C_S C_P}\right)\frac{\partial^2 C}{\partial y^2}$$
$$+ \frac{\mu}{\rho\, C_p}\left(1+\frac{1}{\beta}\right)\left(\frac{\partial u}{\partial y}\right)^2$$

(3)

Mass equation:

$$u\frac{\partial C}{\partial x} + v\frac{\partial C}{\partial y} = D_m\frac{\partial^2 C}{\partial y^2} + \left(\frac{D_m K_T}{T_M}\right)\frac{\partial^2 T}{\partial y^2}$$

(4)

where u and v are velocity components along x and y axes, respectively, ρ is fluid density, υ is kinematic viscosity, μ is dynamic viscosity, $\beta = \mu_B \sqrt{2\pi} / p_y$ is the Casson fluid parameter, σ is the electrical conductivity of the fluid and is assumed to be constant, β_T is the coefficient of thermal expansion, β_C is the coefficient of concentration expansion, T_W is the temperature of the fluid at the stretching sheet, T is the temperature of the fluid within the boundary layer, T_∞ is the temperature of the fluid outside the boundary layer, k is the thermal conductivity of the fluid, C_P is the specific heat at constant pressure p, C_W is the concentration of the fluid at the stretching sheet, C is the concentration of the fluid within the boundary layer, C_∞ is the concentration of the fluid outside the boundary layer, D_M is the chemical molecular diffusivity. Here, g is the acceleration due to gravity.

The applied magnetic field is $B = B_0\, x^{\frac{n-1}{2}}$ where B_0 is assumed to be constant.

Boundary conditions:

$$At\ \ y = 0 : u = cx^n + N_1 \upsilon \left(1 + \frac{1}{\beta}\right)\frac{\partial u}{\partial y}, \quad v = 0,$$

$$\frac{\partial T}{\partial y} = -h_S (T - T_W),\ \frac{\partial C}{\partial y} = -h_C (C - C_W)$$

$$As\ \ y \to \infty : u \to 0,\ ,\ T \to T_\infty\ , C \to C_\infty .$$

(5)

Here $N_1(x) = N\, x^{-\frac{n-1}{2}}$ denotes velocity of slip factor; it depends upon x, and $h_s(x) = h_{T0}\, c\, x^{\frac{n-1}{2}}$ represents the heat transfer parameter for Newtonian heating or temperature slip factor, and $h_c(x) = h_{c0}\, c\, x^{\frac{n-1}{2}}$ is concentration slip factor.

We consider following dimensionless variable to transform the system of Equations (2), (3), (4) and (5) into a dimensionless form:

$$\psi = \left(\frac{2\nu c}{n+1}\right)^{\frac{1}{2}} x^{\frac{n+1}{2}} f(\eta),\ \eta = \left(\frac{c\,(n+1)}{2\nu}\right)^{\frac{1}{2}} x^{\frac{n-1}{2}} y,$$

$$\theta(\eta) = \frac{(T - T_\infty)}{(T_W - T_\infty)}, \phi(\eta) = \frac{(C - C_\infty)}{(C_W - C_\infty)},$$

$$u = \frac{\partial \psi}{\partial y}, v = -\frac{\partial \psi}{\partial x},\ u = cx^n f'(\eta),$$

$$v = -\left(\frac{c\,\upsilon\,(n+1)}{2}\right)^{\frac{1}{2}} x^{\frac{n+1}{2}} \left(f(\eta) + \frac{n-1}{n+1}\eta\, f'(\eta)\right)$$

(6)

Here η is the similarity variable. ψ is stream function. $c\,(c > 0)$ is a parameter related to the surface stretching speed, n is the power index related to the surface stretching speed.

Introducing these variables in the equations we get the following dimensionless forms of the equations:

$$(1 + \frac{1}{\beta}) f''' + f\ f'' + \frac{2n}{n+1} f'^2 + d_1\, \theta + d_2\, \phi$$

$$-(M + (1/K_1)) f' - Fs\left(f'\right)^2 = 0$$

(7)

$$\frac{1}{\Pr}\theta'' + f\,\theta' + \left(1 + \frac{1}{\beta}\right) Ec\, f''^2 = 0$$

(8)

$$\frac{1}{Sc}\phi'' + f\,\phi' + Sr\,\theta'' = 0$$

(9)

With parameters:

$$\left.\begin{aligned}
&M = \frac{2\sigma B_0^2}{\rho c}, K1 = \frac{Kcx^{n-1}}{2\nu}, \Pr = \frac{\upsilon}{\alpha} = \frac{\rho\upsilon C_p}{k} = \frac{\mu C_p}{k},\\
&Gr_T = \frac{2\, g\beta_T (T_W - T_\infty)}{(n+1)c^2\, x^{2n-1}},\ Gr_C = \frac{2\, g\beta_C (C_W - C_\infty)}{(n+1)c^2\, x^{2n-1}},\\
&u = cx^n, Ec = \frac{u^2}{C_p (T_W - T_\infty)} = \frac{c^2 x^{2n}}{C_p (T_W - T_\infty)},\\
&\nu = \frac{\mu}{\rho}, Sc = \frac{\upsilon}{D_m}, Fs = \frac{2bx}{\sqrt{K}}, Du = \frac{D_m\ K_T\ (C_W - C_\infty)}{\upsilon C_S\ C_p\ (T_W - T_\infty)},\\
&Sr = \frac{D_m\ K_T\ (T_W - T_\infty)}{\upsilon T_\infty\ (C_W - C_\infty)}.
\end{aligned}\right\}$$

(10)

Magnetic parameter(Hartmann number)(M), Permeability parameter(K1), Forchheimer parameter(Fs), Prandtl number(Pr), Thermal Grashof

number(Gr_T), Concentration Grashof number(Gr_C), Eckert number(Ec), Dufour number(Du), Schmidth number(Sc) , Soret number(Sr).
And corresponding boundary conditions as follows:

$$f(0)=0,\ f'(0)=1+\delta\left(1+\frac{1}{\beta}\right)$$
$$f''(0), \theta'(0)=-\gamma_1[1+\theta(0)],$$
$$\phi'(0)=-\gamma_2[1+\phi(0)]$$
$$f'(\infty)=0,\ \theta(\infty)=0, \phi(\infty)=0$$
(11)

where

$$N=N_1 x^{-\frac{n-1}{2}}, \delta=N\left(\frac{(n+1)c\upsilon}{2}\right)^{\frac{1}{2}},$$

$$h_T=h_{T0}\, c\, x^{\frac{n-1}{2}}, \gamma_1=h_{T0}\left(\frac{2\upsilon}{c(n+1)}\right)^{\frac{1}{2}}$$

$$h_C=h_{C0}\, c\, x^{\frac{n-1}{2}}, \gamma_1=h_{C0}\left(\frac{2\upsilon}{c(n+1)}\right)^{\frac{1}{2}}$$
(12)

δ is called velocity slip parameter, γ_1 is called thermal slip parameter, and γ_2 is called concentration slip parameter.

The physical quantities of Engineering interest are the skin friction coefficient (rate of shear stress), the couple stress coefficient at the sheet the Nusselt number (rate of heat transfer), and the Sherwood number (rate of mass transfer).

The local Skin-friction C_f, local Nusselt Number Nu_x and local Sherwood Number Sh_x which are defined as

$$\left.\begin{aligned}
C_f &= \frac{\tau_w}{\frac{\rho U_w^2}{2}}=\frac{\mu_B\left(1+\frac{1}{\beta}\right)\left(\frac{\partial u}{\partial y}\right)_{y=0}}{\frac{\rho U_w^2}{2}}\\
\Rightarrow C_f &= \left(\frac{2\nu(n+1)}{c}\right)^{\frac{1}{2}} x^{-\frac{(n+1)}{2}} f''(0),\\
C_f &= \left(\frac{2(n+1)}{\mathrm{Re}}\right)^{\frac{1}{2}}\left(1+\frac{1}{\beta}\right) f''(0),\\
\mathrm{Re} &= \frac{cx^{(n+1)}}{\nu}.
\end{aligned}\right\}$$
(13)

Here $-\left(\frac{\partial T}{\partial y}\right)_{y=0}$ is a heat flux from the surface of the sheet and Re is the local Reynold Number.

$$\left.\begin{aligned}
Sh &= -\frac{x\left(\frac{\partial C}{\partial y}\right)_{y=0}}{C_w-C_\infty}=-\left(\frac{c(n+1)}{2\nu}\right)^{\frac{1}{2}} x^{\frac{(n+1)}{2}}\phi'(0),\\
Sh &= -\left(\frac{(n+1)cx^{(n+1)}}{2\nu}\right)^{\frac{1}{2}}\phi'(0)=-\left(\frac{(n+1)}{2}\mathrm{Re}\right)^{\frac{1}{2}}\phi'(0).
\end{aligned}\right\}$$
(14)

Here $-\left(\frac{\partial C}{\partial y}\right)_{y=0}$ is a mass flow rate from the surface of the sheet and Re is the local Reynold Number.

III. METHOD OF NUMERICAL SOLUTION

The numerical solutions are obtained using the equations (7)-(9) and boundary conditions (11) for some values of the governing parameters, namely, Casson fluid parameter b, magnetic parameter M, Darcy parameter Da, Forchheimer parameter Fs. Effects of b, M, Da, and Fs on the steady boundary layer flow are discussed in detail. The numerical computation is done using the MATLAB in-built Numerical Solver bvp4c. In the computation we have taken $\eta_\infty=10$ and axis according to the clear figure-visuality.

IV. RESULT ANALYSIS AND DISCUSSION

In order to analyze the behaviour of non-dimensional linear velocity $f'(\eta)$, temperature $\theta(\eta)$, and concentration $\phi(\eta)$ profiles of the physical problem, numerical calculations are carried out for various values of Casson fluid parameter b, magnetic parameter M, Darcy parameter Da, Forchheimer parameter Fs. Also, the skin friction factor and Nusselt and Sherwood numbers are discussed . For illustrations of the results, the numerical data are tabulated in tables 1-8 and plotted in Figs. 2–10.

The results for skin friction and local Nusselt number are compared with the previous published results, and are shown in Tables 1–2. It is observed that the obtained results are in good agreement with the published results.

Tables 1 and 2 present the values of skin friction coefficient and reduced Nusselt number for different values of nonlinear stretching parameter n and Prandtl number Pr, respectively. The present results are compared with the results of Cortell (2007) and Ullah et al.(2016). It is also observed from Table 1 that magnitude of skin friction coefficient $\left|\left(1+\frac{1}{b}\right)f''(0)\right|$ increases with the increase in n whereas reduced Nusselt number decreases with the increase in n and increases with increase in Pr (Table 2).

For the convenience in calculation in Matlab following symbles are used for respective symbols used in modelling equations and boundary conditions:

$$a1 = f''(0),\ a2 = \theta'(0),\ a3 = \phi'(0),$$

$$d = \delta,\ d1 = Gr_T,\ d2 = Gr_C,\ b = \beta,$$

$$m1 = \gamma_1,\ m2 = \gamma_2,\ n1 = n.$$

Table 1 Comparison of $f''(0)$ for different values of n1 with Fs=0.0, d1=0.0, d2=0.0, d=0.0, m1=10.^ 4, m2=10.^ 4 ,M=0, Pr=1.00, Du=0.0, Sc=0.22, a1=0.0, a2=1.0, a3=1.0, b=10.^8, Ec=0.0, Da=10^7, Sr=0.

$f''(0)$			
n1	Cortell(2007)	Ullah et al.(2016)	Present
0.0	0.627547	0.6276	0.627631963479766
0.2	0.766758	0.7668	0.766906263551595
0.5	0.889477	0.8896	0.889594172073448
1	1.0	1.0	1.000062567556568
3	1.148588	1.1486	1.148660394543063
10	1.234875	1.2349	1.234952969673218
100	1.276768	1.2768	1.276830449563257

Table 2 Comparison of local Nusselt number $-\theta'(0)$ for various values of Pr and n1 with Fs=0.0, d1=0.0, d2=0.0, d=0.0, m1=10.^4, m2=10.^4, M=0, Pr=1.00, Du=0.0, Sc=0.22, a1=0.0, a2=1.0, a3=1.0, b=10.^8, Ec=0.0, Da=10.^ 7, Sr=0.

$-\theta'(0)$,Pr=1,			
n1	Cortell(2007)	Ullah et al.(2016)	Present
0.2	0.610262	0.6102	0.610277445039946
0.5	0.595277	0.5949	0.595283487517005
1.5	0.574537	0.5747	0.574829838650739
3.0	0.564472	0.5647	0.564775152915357

Values of parameters for tables 3-8:

Table 3 n1=2, M=1.0, Da=10.0, Fs=0.5, d1=0.50, d2=0.50, Pr=0.71, Ec=0.5, Du=0.10, Sc=0.2, Sr=0.7, a1=1.0, d=0.2, m1=10.^4, a2=1.0, m2=10.^4, a3=1.0, b=[0.1;0.2;0.3;0.5].

$\lvert(1+1/b)f''(0)\rvert$			
b	M=1	M=5	M=10
0.1	-2.57217203854863	-2.79039160311035	-3.0426335570851
0.2	-2.154973004665859	-2.38031718849103	-2.63710319559902
0.3	-2.051386466471404	-2.28678361261042	-2.55315452085676
0.5	-2.014577874610683	-2.2680729007147	-2.63710319559902

Table 4

$-\theta'(0)$			
b	M=1	M=5	M=10
0.1	-9.9727440051193	-11.251683	-12.7510763730
0.2	-3.0243367042252	-3.5596444	-4.17826174755
0.3	-1.6104454211498	-1.9700216	-2.38208478152
0.5	-0.7711608688806	-1.0164968	-4.17826174755

Table 5

$-\phi'(0)$			
b	M=1	M=5	M=10
0.1	-0.848489696715858	-1.0331804204707	-1.250046784930789
0.2	-0.080077730352126	-0.1675488223871	-0.267498305735198
0.3	0.057984443470540	-0.0053590980562	-0.076291750113559
0.5	0.130706429521058	0.0837981774664	-0.267498305735198

Table 6

$\lvert(1+1/b)f''(0)\rvert$						
b	Da=0.1	Da=0.5	Da=1.0	Fs=0.5	Fs=2.5	Fs=3.5
0.1	-2.5722	-2.0735	-2.0032	-1.9379	-2.2338	-2.3695
0.2	-2.1550	-1.6237	-1.5462	-1.4734	-1.7030	-1.8083
0.3	-2.0514	-1.4877	-1.4039	-1.3249	-1.5384	-1.6362
0.5	-2.0146	-1.3970	-1.3036	-1.2149	-1.4228	-1.5179

Table 7

$-\theta'(0)$						
b	Da=0.1	Da=0.5	Da=1.0	Fs=0.5	Fs=2.5	Fs=3.5
0.1	-9.9727	-7.1254	-6.7338	-6.3731	-7.5432	-8.0990
0.2	-3.0243	-1.7989	-1.6254	-1.4639	-1.8197	-1.9888
0.3	-1.6104	-0.7759	-0.6564	-0.5449	-0.7531	-0.8521
0.5	-0.7712	-0.1914	-0.1073	-0.0288	-0.1546	-0.2144

Table 8

$-\phi'(0)$						
b	Da=0.1	Da=0.5	Da=1.0	Fs=0.5	Fs=2.5	Fs=3.5
0.1	-0.8485	-0.4388	-0.3826	-0.3310	-0.5025	-0.5837
0.2	-0.0801	0.1239	0.1532	0.1805	0.1208	0.0928
0.3	0.0580	0.2114	0.2343	0.2558	0.2171	0.1991
0.5	0.1307	0.2502	0.2689	0.2867	0.2603	0.2481

Table 3-5 shows for fixed value of Csson parameter, with the increase in magnetic parameter skin friction, Nusselt number and Sherwood number decreases. For fixed value of magnetic parameter, with the increase in Casson fluid parameter skin friction, Nusselt number and Sherwood number increases.

Table 6-8 shows for fixed value of Csson parameter, with the increase in Darcy parameter skin friction, Nusselt number and Sherwood number increases. While with the increase in the value of Forchheimer number skin friction Nusselt number and Sherwood number decreases.

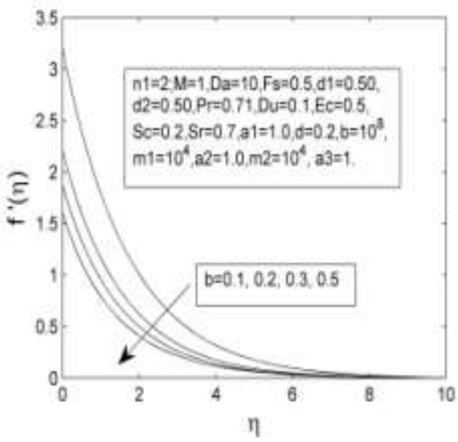

Figure 2 Velocity profile $f'(\eta)$ with respect to similarity transformation η for some values of Casson parameter b.

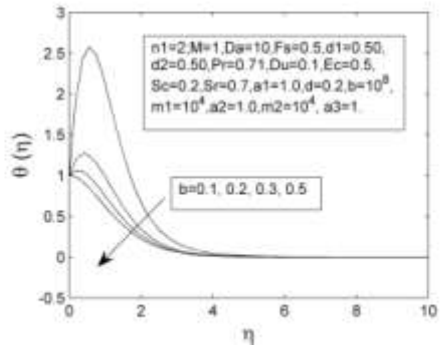

Figure 3 Temperature profile $\theta(\eta)$ with respect to η for some values of Casson parameter b.

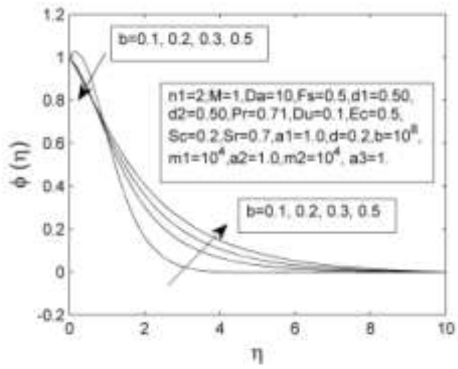

Figure 4 Concentration profile $\phi(\eta)$ with respect to η for some values of Casson parameter b.

Fig.2-4 show effect of Casson parameter on velocity, temperature and concentration profiles.

From Fig.1, non-dimensional velocity decreases with the increase in the value of similarity transformation η. Also, velocity profile decreases with the increase in the value of Casson parameter b. This shows velocity boundary layer thickness decreases with the increase in the value of Casson parameter b.

From Fig.2, non-dimensional temperature increases in the range about [0, 1] and then begins to decrease with the increase in the value of similarity transformation η about [1, 10]. Also, temperature profile decreases with the increase in the value of Casson parameter b. This shows thermal boundary layer thickness decreases with the increase in the value of Casson parameter b.

From Fig.3, non-dimensional concentration increases in the range about [0, 1] and then begins to decrease with the increase in the value of similarity transformation η about [1, 10]. Also, concentration profile decreases with the increase in the value of Casson parameter b. This shows concentration boundary layer thickness decreases with the increase in the value of Casson parameter b.

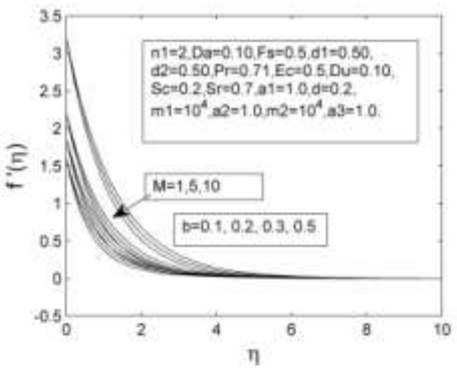

Figure 5 Velocity profile $f'(\eta)$ with respect to similarity transformation η for some values of Casson parameter b and magnetic parameter M.

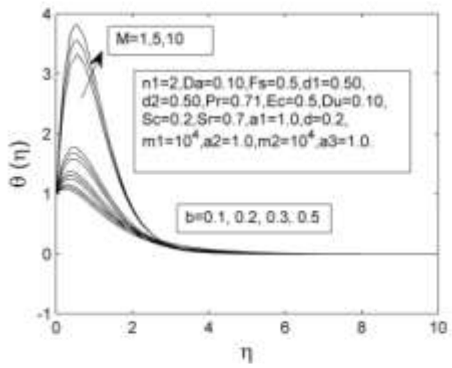

Figure 6 Temperature profile $\theta(\eta)$ with respect to η for some values of Casson parameter b and magnetic parameter M.

Fig.5-6 show effect of magnetic parameter and Casson parameter on velocity, temperature and concentration profiles.

From Fig.5, non-dimensional velocity decreases with the increase in the value of similarity transformation η. Also, velocity profile decreases with the increase in the value of magnetic parameter keeping Casson parameter b fix. This shows velocity boundary layer thickness decreases with the increase in the value of magnetic parameter, keeping Casson parameter b fix.

From Fig.6, non-dimensional temperature increases in the range about [0, 1] and then begins to decrease with the increase in the value of similarity transformation η about [1, 10]. Also, temperature profile increases with the increase in the value of magnetic parameter keeping Casson parameter b fix. This shows thermal boundary layer thickness increases with the increase in the value of magnetic parameter, keeping Casson parameter b fix.

Also, concentration profile does not show any change with the increase in the value of magnetic parameter, keeping Casson parameter b fix. This shows concentration boundary layer thickness is not affected with the increase in the value of magnetic parameter keeping Casson parameter b fix.

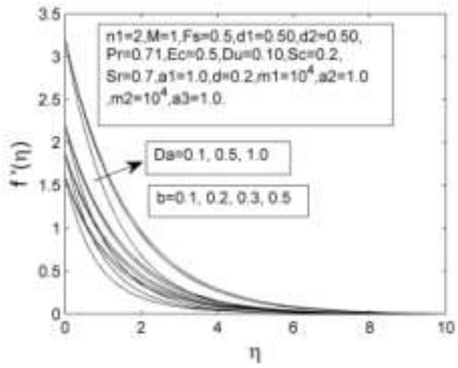

Figure 7 Velocity profile $f'(\eta)$ with respect to similarity transformation η for some values of Casson parameter b and Darcy parameter Da.

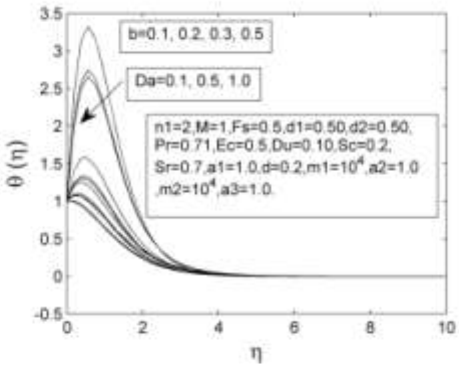

Figure 8 Temperature profile $\theta(\eta)$ with respect to η for some values of Casson parameter b and Darcy parameter Da.

From Fig.7 the velocity profile increases with the increase in the value of Darcy parameter Da, keeping Casson parameter b fix. This shows velocity boundary layer thickness increases with the increase in the value of Darcy parameter Da.

From Fig.8 the temperature profile decreases with the increase in the value of Darcy parameter Da, keeping Casson parameter b fix. This shows velocity boundary layer thickness decreases with the increase in the value of Darcy parameter Da.

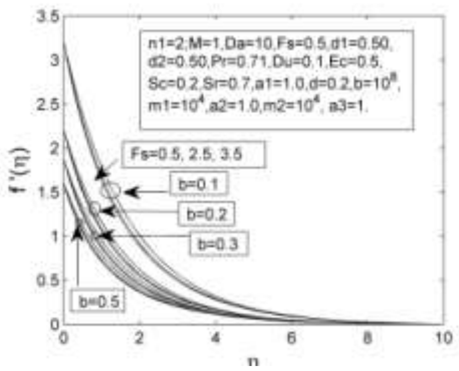

Figure 9 Velocity profile $f'(\eta)$ with respect to similarity transformation η for some values of Casson parameter b and Forchheimer parameter Fs.

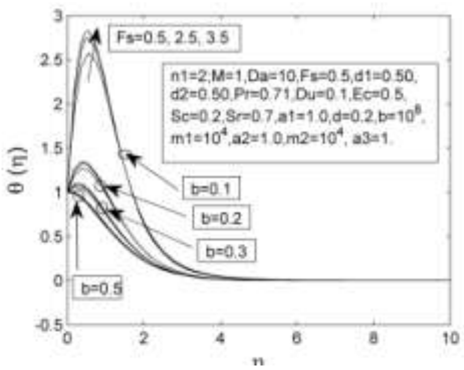

Figure 10 Temperature profile $\theta(\eta)$ with respect to η for some values of Casson parameter b and Forchheimer parameter Fs.

From Fig.9 the velocity profile decreases with the increase in the value of Forchheimer parameter Fs, keeping Casson parameter b fix. This shows velocity boundary layer thickness decreases with the increase in the value of Forchheimer parameter Fs.

From Fig.10 the temperature profile increases with the increase in the value of Forchheimer parameter Fs, keeping Casson parameter b fix. This shows velocity boundary layer thickness increases with the increase in the value of Forchheimer parameter Fs.

V. CONCLUSION

In the present paper the numerical study of the effect of Darcy and Forchheimer parameters on Magnetohydrodynamic Casson fluid flow is explored. By suitable similarity transformations, the governing boundary layer equations are transformed to ordinary differential equations and to solve these equations the method applied is numerical computation with bvp4c, a MATLAB program. The effects of Casson fluid parameter,Magnetic Parameter, Darcy Parameter, and Forcheimer parameter on velocity, heat transfer, and concentration profiles, Skin- Frictions, Nusselt Number and Sherwood Number are computed and discussed numerically and presented through tables and graphs.

From the above work following results are concluded.

Non-dimensional Velocity decreases with the increase in the value of similarity variable.

Non-dimensional temperature increases in the range about [0, 1] and then begins to decrease with the increase in the value of similarity transformation η in about [1, 10].

Non-dimensional concentration increases in the range about [0, 1] and then begins to decrease with the increase in the value of similarity transformation η in about [1, 10].

Velocity profiles decrease with the increase in Magnetic parameters. And hence Velocity, boundary layer thicknesses decreases.

Temperature profiles increase with the increase in Magnetic parameters. And hence temperature boundary layer thicknesses increases.

Velocity, temperature and concentration profiles decrease with the increase in Casson fluid parameter. And hence Velocity, temperature, and concentration boundary layer thicknesses decreases.

Velocity profiles increase with the increase in Darcy parameters. And hence Velocity, boundary layer thicknesses increases.

Temperature profiles decrease with the increase in Darcy parameters. And hence temperature boundary layer thicknesses decreases.

Velocity profiles decrease with the increase in Forchheimer parameters. And hence Velocity, boundary layer thicknesses decreases.

Temperature profiles increase with the increase in Forchheimer parameters. And hence temperature boundary layer thicknesses increases.

Table 3-5 shows for fixed value of Csson parameter, with the increase in magnetic parameter skin friction, Nusselt number and Sherwood number decreases. For fixed value of magnetic parameter , with the increase in Casson fluid parameter skin friction, Nusselt number and Sherwood number increases.

Table 6-8 shows for fixed value of Csson parameter, with the increase in Darcy parameter skin friction, Nusselt number and Sherwood number increases. While with the increase in the value of Forchheimer number skin friction Nusselt number and Sherwood number decreases.

COMPETING INTERESTS

The author declares that he has no competing interest.

ACKNOWLEDGEMENT

I am thankful to Asst. Prof. Dr. Saravanan Department of Computer Science, for his help and advice and the Department of Mathematics, K.L. University, Guntur, A. P. for the support during the preparation of the paper.

REFERENCE

1. Casson N. In: Mill CC, editor. A Flow Equation for Pigment Oil-Suspensions of the Printing Ink Type. Rheology of Disperse Systems, 84.Pergamon Press; 1959.
2. Bird RB, Dai GC, Yarusso BJ. The rheology and flow of viscoplastic materials. Rev Chem Eng 1983; 1:1–83.
3. B.C. Sakiadis, Boundary layer behavior on continuous solid surfaces: II. The boundary layer on continuous flat surface, AIChE J. 7 (1961) 221–225.
4. L.J. Crane, Flow past a stretching plane, Z. Angew. Math. Phys.21 (1970) 645–647.
5. Nield, D.A. and A. Bejan, A. (1999). Convection in porous media. 2nd ed. Springer, New York.
6. Mukhopadhyay, Swati.Casson fluid flow and heat transfer over a nonlinearly stretching surface. Chin. Phys. B Vol. 22, No. 7 (2013) 074701.DOI: 10.1088/1674-1056/22/7/074701.
7. M. Mustafa and Junaid Ahmad Khan. Model for flow of Casson nanofluid past a non-linearly stretching sheet considering magnetic field effects. AIP Advances 5, 077148 (2015); http://dx.doi.org/10.1063/1.4927449.
8. Medikare, M., Joga, S. and Chidem, K.K. (2016) MHD Stagnation Point Flow of a Casson Fluid over a Nonlinearly Stretching Sheet with Viscous Dissipation. *American Journal of Computational Mathematics*, **6**, 37-48. http://dx.doi.org/10.4236/ajcm.2016.61005.
9. S. Pramanik. Casson fluid flow and heat transfer past an exponentially porous stretching surface in presence of thermal radiation. Ain Shams Engineering Journal (2014) 5, 205–212. http://dx.doi.org/10.1016/j.asej.2013.05.003.
10. C.S.K. Raju, N. Sandeep, V. Sugunamma , M. Jayachandra Babu, J.V. Ramana Reddy. Heat and mass transfer in magnetohydrodynamic Casson fluid over an exponentially permeable stretching surface. Engineering Science and Technology, an International Journal 19 (2016) 45–52. http://dx.doi.org/10.1016/j.jestch.2015.05.010.
11. Saidulu, N. and A Venkata Lakshmi. Slip Effects on MHD Flow of Casson Fluid over an Exponentially Stretching Sheet in Presence of Thermal Radiation, Heat Source/Sink and Chemical Reaction .European Journal of Advances in Engineering and Technology, 2016, 3(1): 47-55.
12. Sharada, K. and Shankar, B. MHD Mixed Convection Flow of a Casson Fluid over an Exponentially Stretching Surface with the Effects of Soret, Dufour, Thermal Radiation and Chemical Reaction. *World Journal of Mechanics*, 2015, **5**, 165-177. http://dx.doi.org/10.4236/wjm.2015.59017.
13. Swati Mukhopadhyay, Krishnendu Bhattacharyya, and Tasawar Hayat. Exact solutions for the flow of Casson fluid over a stretching surface with transpiration and heat transfer effects. Chin. Phys. B Vol. 22, No. 11 (2013) 114701. DOI: 10.1088/1674-1056/22/11/114701.
14. Hayat T, Shehzadi SA, Alsaedi A. Soret and Dufour effects on magnetohydrodynamic (MHD) flow of Casson fluid. Appl Math Mech (English Ed.) 2012;33(10):1301–12.
15. Mahdy, A. Heat transfer and flow of a Casson fluid due to a stretching cylinder with the Soret and Dufour effects. *Journal of Engineering Physics and Thermophysics,* Vol. 88, No. 4, July, 2015.
16. I.L. Animasaun . Effects of thermophoresis, variable viscosity and thermal conductivity on free convective heat and mass transfer of non-darcian MHD dissipative Casson fluid flow with suction and nth order of chemical reaction. Journal of the Nigerian Mathematical Society 34 (2015) 11–31. http://dx.doi.org/10.1016/j.jnnms.2014.10.008.
17. Imran Ullah, Sharidan Shafie, Ilyas Khan , Effects of slip condition and Newtonian heating on MHD flow of Casson fluid over a nonlinearly stretching sheet saturated in a porous medium.Journal of King Saud University –Science. j.jksus.2016.05.003;http://dx.doi.org/10.1016.
18. Butt, A. S., M. N. Tufail, and Asif Ali. Three-dimensional flow of a magnetohydrodynamic Casson fluid over an unsteady stretching sheet embedded into a porous medium. *ISSN 0021-8944, Journal of Applied Mechanics and Technical Physics, 2016, Vol. 57, No. 2, pp. 283–292.* c_ *Pleiades Publishing, Ltd., 2016.*
19. S. A. Shehzad, T. Hayat, M. Qasim and S. Asghar. Effects of mass transfer on mhd flow of Casson fluid with chemical reaction and suction. Brazilian Journal of Chemical Engineering, Vol. 30, No. 01, pp. 187 - 195, January - March, 2013.
20. Arthur, E.M., Seini, I.Y. and Bortteir, L.B. Analysis of Casson Fluid Flow over a Vertical Porous Surface with Chemical Reaction in the Presence of Magnetic Field. *Journal of Applied Mathematics and Physics*, (2015) **3**, 713-723.http://dx.doi.org/10.4236/jamp.2015.36085.
21. Hussanan,Abid., Mohd Zuki Salleh, Razman Mat Tahar, Ilyas Khan. Unsteady Boundary Layer Flow and Heat Transfer of a Casson Fluid past an Oscillating Vertical Plate with Newtonian Heating. PLOS ONE : October 2014 | Volume 9 | Issue 10 | e108763| www.plosone.org.
22. Kirubhashankar, C. K., S. Ganesh and A. Mohamed Ismail.Casson Fluid Flow and Heat Transfer over an Unsteady Porous Stretching Surface . Applied Mathematical Sciences, Vol. 9, 2015, no. 7, 345 – 351. http://dx.doi.org/10.12988/ams.2015.411988.
23. Motahar Reza, Rajni Chahal, Neha Sharma. Radiation Effect on MHD Casson Fluid Flow over a Power-Law Stretching Sheet with Chemical Reaction. World Academy of Science, Engineering and Technology International Journal of Chemical, Molecular, Nuclear, Materials and Metallurgical Engineering Vol:10, No:5, 2016.
24. Siddiqui, A. M., A. A. Farooq, and M. A. Rana. A Mathematical Model for the Flow of a Casson Fluid due to Metachronal Beating of Cilia in a Tube.Hindawi Publishing Corporation□e Scientific World Journal Volume 2015, Article ID 487819, 12 pages http://dx.doi.org/10.1155/2015/487819.
25. Shaw, Sachin., Ganeswar Mahanta , Precious Sibanda. Non-linear thermal convection in a Casson fluid flow over a horizontal plate with convective boundary condition. Alexandria Engineering Journal (2016) 55, 1295–1304. http://dx.doi.org/10.1016/j.aej.2016.04.020.
26. Rao AS, Prasad VR, Reddy NB, B´eg OA. Heat Transfer in a Casson Rheological Fluid from a Semi-infinite Vertical Plate with Partial Slip, Wiley Periodicals, Inc. Heat Trans Asian Res; Published online in Wiley Online Library. (wileyonlinelibrary.com/journal/htj),http://dx.doi.org/10.100 2/htj.21115, 2013.
27. Forchheimer PZ. Wasserbewegung Durch Boden. Zeit Ver Deutsch Ing 1901; 45:1781–8.
28. Darcy H. Les fontainer publigues de la ville de Dijoin. Dalmont; 1856.